Communications In Catalysis
Vol. 3, No. 1, 2026, pp. 1-12
DOI: 10.22049/cic.2026.31717.1042
Azarbaijan Shahid Madani University

Surface-Modified B, N-Co-Doped Carbon Quantum Dots for PEG-Based Lubricants: Synthesis, Physicochemical Characterization, and Antioxidant Activity

Fatemeh Emamali Sabzi[1*]. Mehrdad Mahkam[2]

[1,2]Chemistry Department, Faculty of Science, Azarbaijan Shahid Madani University, Tabriz, Iran

Email: emamalisabzi.fatemeh@gmail.com

Received: 2026-03-24, Accepted: 2026-04-10

Abstract: Lubricating oils are widely used to reduce friction, wear, and energy loss between moving surfaces. In recent years, carbon quantum dots (CQDs) have attracted considerable attention as lubricant additives because of their low toxicity, environmental compatibility, thermal stability, and tunable surface chemistry. In this study, boron- and nitrogen-co-doped carbon quantum dots (BNCQDs) were synthesized through a simple one-step pyrolysis of diethanolamine, citric acid, and boric acid and evaluated as additives in polyethylene glycol (PEG). The synthesized BNCQDs were characterized by ^{1}H NMR, TGA, XRD, FT-IR, and fluorescence spectroscopy. Their antioxidant activity and key lubricant-related properties, including flash point, pour point, and kinematic viscosity, were also investigated. The results confirmed the successful incorporation of boron and nitrogen into the CQD structure and demonstrated favorable thermal, optical, and antioxidant characteristics. These findings indicate that BNCQDs have promising potential as multifunctional and environmentally friendly additives for improving the performance of PEG-based lubricants.

Keywords: Boron-nitrogen co-doped carbon quantum dots; Nano-lubricant additives; Polyethylene glycol; Antioxidant activity; Thermal stability; Tribology

1.Introduction

Friction and wear in mechanical systems are major sources of energy loss, component failure, and environmental burden. In internal-combustion engines and industrial machinery, inadequate lubrication increases fuel consumption, accelerates surface degradation, and shortens service life [1, 2]. Effective lubrication is therefore essential for separating contacting surfaces, reducing frictional losses, dissipating heat, and protecting components against wear and corrosion. The development of high-performance lubricants and multifunctional additives is consequently an important strategy for improving energy efficiency and operational reliability [3, 4].

Base oils alone generally cannot satisfy the demanding thermal, oxidative, and tribological requirements of modern machinery [5]. Lubricant additives are therefore incorporated to modify viscosity, suppress oxidation and corrosion, reduce friction and wear, and promote the formation of protective boundary films. Depending on the application, additive packages may constitute a substantial fraction of the final lubricant formulation [6, 7]. However, many conventional additives contain sulfur, phosphorus, or metals and may generate environmentally undesirable by-products. This has increased interest in low-toxicity, metal-free, and environmentally compatible nanomaterials that can provide multiple functions at relatively low concentrations.

Among emerging nanomaterials, carbon quantum dots (CQDs) have attracted particular attention. CQDs are quasi-spherical, zero-dimensional carbon nanoparticles, typically smaller than 10 nm, consisting of carbonaceous cores and abundant surface functional groups [8]. They exhibit high chemical and thermal stability, tunable surface chemistry, good dispersibility, low toxicity, and relatively simple and inexpensive synthesis. Since their discovery, CQDs have been investigated in sensing, bioimaging, catalysis, photovoltaics, and other advanced applications [7]. Their small size, surface activity, and capacity to form stable interfacial films also make them promising nano-additives for tribological systems [9, 10]. The tribological performance of CQDs is strongly influenced by their composition, surface functionality, and compatibility with the base lubricant [11]. Appropriate functionalization can improve dispersion stability and facilitate adsorption on contacting metal surfaces, where the nanoparticles may form a protective film, fill surface asperities, and reduce direct metal-to-metal contact [12-14]. These mechanisms can decrease friction and wear while enhancing the thermal and oxidative stability of the lubricant. Nevertheless, the practical application of CQDs remains dependent on controlling their surface chemistry and maintaining stable dispersion under operating conditions [15, 16].

Heteroatom doping is an effective approach for tailoring the electronic, optical, and chemical properties of CQDs. Boron- and nitrogen-containing compounds are widely used in tribology as friction modifiers, antioxidants, and antiwear additives [14]. Because boron is electron-deficient and susceptible to hydrolysis, interactions with electron-rich nitrogen atoms can stabilize

boron-containing structures and improve their interfacial activity [14, 17]. Co-doping CQDs with boron and nitrogen may therefore combine the favorable characteristics of carbon nanodots with the lubricating and antioxidant functions associated with B-N-containing compounds [18].

In this study, boron- and nitrogen-co-doped carbon quantum dots (BNCQDs) were synthesized from citric acid, boric acid, and diethanolamine through a simple one-step thermal process. Diethanolamine served as the nitrogen source and also provided surface functionalities relevant to corrosion inhibition and lubricant compatibility [19-21]. The synthesized BNCQDs were subsequently modified with oleic acid and stearic acid to improve their compatibility with lubricant media. Their structural, thermal, and optical properties were investigated by FT-IR, XRD, ^{1}H NMR, TGA, and fluorescence spectroscopy. Antioxidant performance and key lubricant-related properties, including flash point, pour point, and kinematic viscosity, were also evaluated to assess their potential as multifunctional and environmentally compatible additives for PEG-based lubricants.

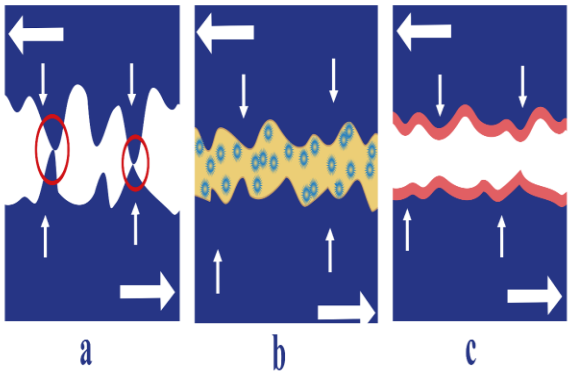

Scheme 1. Schematic illustration of the lubrication mechanism: (a) direct contact between unlubricated surfaces, leading to friction, wear, and surface damage; (b) separation of the contacting surfaces by a lubricant containing functional additives; and (c) adsorption of lubricant additives onto the metal surfaces, forming a protective film that reduces friction, wear, and chemical attack.

2. Materials and methods

2.1. Materials & apparatus measurements

Boric acid (H_3BO_3), diethanolamine [$HN(CH_2CH_2OH)_2$], oleic acid ($C_{18}H_{34}O2$), and stearic acid ($C_{18}H_{36}O_2$) were purchased from Merck and used without further purification. Proton nuclear magnetic resonance (^{1}H NMR) spectra were recorded in $CDCl_3$ using a Bruker FT-NMR spectrometer operating at 400 MHz. Fourier-transform infrared (FT-IR) spectra were obtained using a Bruker Vector 22 spectrophotometer. Powder X-ray diffraction (XRD) patterns were recorded with a Bruker D8 Advance diffractometer using Cu Kα radiation (λ = 0.154056 nm). Thermogravimetric analysis (TGA) was performed using a Mettler Toledo instrument under a nitrogen atmosphere at a heating rate of 10 ℃ min^{-1}. Fluorescence emission spectra

and intensity measurements were obtained using an FP-6200 spectrofluorometer (JASCO Corporation, Tokyo, Japan). Antioxidant activity was evaluated using a BioTek UV–Vis spectrophotometer. The flash point was measured using a Cleveland open-cup flash-point apparatus (PT-1015). Cloud and pour points were determined according to the relevant ASTM procedures using a cloud- and pour-point analyzer. Kinematic viscosity was measured using a digital precision viscosity bath (PT-2115).

2.2. Preparation and synthesis of BNCQD

Boron- and nitrogen-co-doped carbon quantum dots (BNCQDs) were synthesized through a one-step thermal treatment. Diethanolamine (15 mL), boric acid (5 g), and citric acid (5 g) were mixed in a beaker and stirred vigorously using a magnetic stirrer until a homogeneous mixture was obtained. The reaction mixture was then heated at 120 ℃ for 6 h. During the thermal treatment, dehydration and condensation reactions occurred among the precursor molecules, promoting carbonization and the formation of the BNCQD structure. The gradual color change of the reaction mixture from white to pale yellow, yellow, orange, red, and finally dark red indicated the progress of the carbonization process. After completion of the reaction, the resulting BNCQD product was cooled to room temperature and collected for subsequent characterization and further modification.

2.3. synthesis BNCQD-OL

Oleic acid-modified boron- and nitrogen-co-doped carbon quantum dots (BNCQD-OL) were prepared through a surface esterification process. A three-neck round-bottom flask equipped with a mechanical stirrer, thermometer, reflux condenser, and Dean-Stark trap was charged with toluene (150 mL), oleic acid (60 g), and the previously synthesized BNCQDs. The reaction mixture was heated to 110 ℃ and refluxed for 3 h under continuous mechanical stirring. Water generated during the esterification reaction was continuously removed using the Dean-Stark trap to shift the reaction toward product formation. After completion of the reaction, residual toluene and water were removed under reduced pressure. The resulting product was obtained as a white, paraffin-like material and designated BNCQD-OL.

2.4. Synthesis BNCQD-ST

Oxidation is one of the principal causes of lubricant degradation. Oxidative reactions generate acidic and polymeric products that may increase oil viscosity, promote sludge and varnish formation, accelerate corrosion, and impair the cooling and friction-reducing performance of the lubricant [8–10]. Antioxidant additives are therefore employed to inhibit free-radical oxidation reactions and improve the oxidative stability and service life of lubricating oils. The antioxidant activity of the synthesized BNCQDs was evaluated using the 2,2-diphenyl-1-picrylhydrazyl (DPPH) free-radical scavenging assay. This spectrophotometric method is based on the reduction of the stable DPPH radical by antioxidant species, which results in a decrease in absorbance at 517 nm [22].

To prepare the calibration curve, DPPH solutions with concentrations of 140, 160,

and 200 mg L^{-1} were prepared in methanol. The freshly prepared solutions were incubated in the dark for 30 min, after which their absorbance was measured at 517 nm using methanol as the blank. A calibration curve was constructed by plotting DPPH concentration against absorbance at 517 nm [14]. The linear regression equation obtained from the calibration curve was subsequently used to determine the residual DPPH concentration in the BNCQD-containing samples. The correlation obtained by the linear regression for the DPPH standard curve BNCQDs are shown in Fig.1. The remaining DPPH values were determined using the DPPH standard curve that was developed. The remaining DPPH percentages were then computed using the following formula:

$$DPPH_{rem} = (DPPH_{30}/DPPH_0) \times 100\%$$

Where DPPH0 represents the initial concentration of DPPH free radicals and DPPH30 represents the DPPH free radical concentration after thirty minutes. Results are presented in the form of residual concentrations of DPPH as obtained from a calibration curve [23, 24].

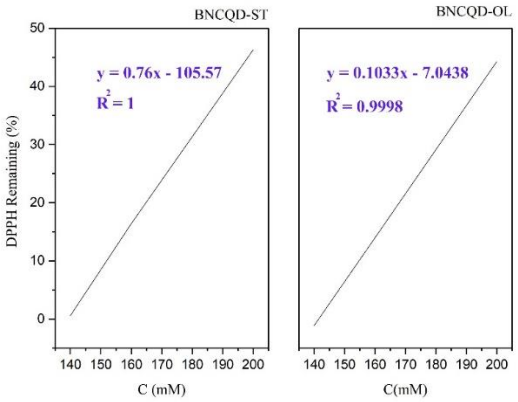

Figure 1. The standard curve of DPPH concentration against absorbance at 517 nm.

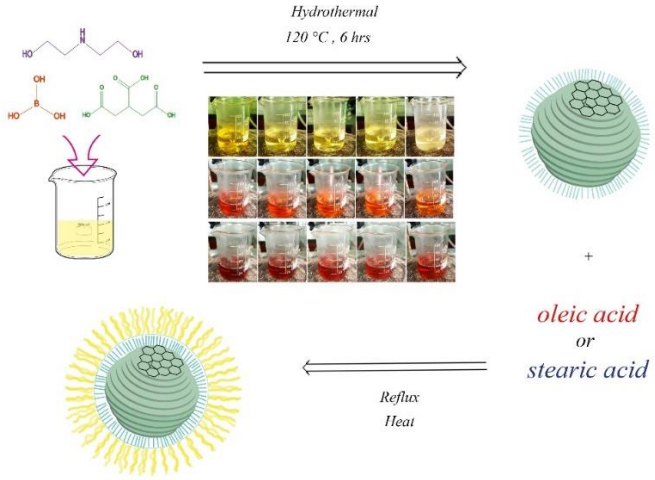

Scheme 2. Schematic illustration for the preparation of BNCQDs

3. Results and discussion

3.1. FT-IR

The formation and surface functionalization of the synthesized BNCQDs were investigated by Fourier-transform infrared spectroscopy. The FT-IR spectra showed characteristic absorption bands associated with B-N, N-H, O-H, C-O, B-O, and B-C bonds, confirming the successful incorporation of boron- and nitrogen-containing functional groups into the carbon-dot structure. For BNCQD-OL, a broad

absorption band in the range of 3100–3500 cm^{-1} was assigned to the overlapping stretching vibrations of O-H and N-H groups. The presence of these polar surface functionalities contributes to the hydrophilic character of the synthesized BNCQDs [22]. The C-H stretching vibration was observed at approximately 2750 cm^{-1}, while the absorption band at 1705 cm^{-1} was attributed to the stretching vibration of carbonyl (C=O) groups. In addition, the band located near 1080 cm^{-1} was assigned to C-O stretching [25].

The characteristic absorption bands at approximately 1480 and 1280 cm^{-1} were attributed to B-O and B-C stretching vibrations, respectively, providing evidence for the successful incorporation of boron into the BNCQD-OL structure. Furthermore, the bands observed at approximately 1350 and 800 cm^{-1} were assigned to B-N stretching and B-N-B bending vibrations, respectively, indicating the presence of nitrogen-containing boron species within the synthesized material. The FT-IR spectrum of BNCQD-ST also exhibited characteristic bands at approximately 1349, 1480, and 1618 cm^{-1}, which were associated with B-N-related vibrational modes. A broad absorption band between 3100 and 3500 cm^{-1} was again attributed to O-H and N-H stretching vibrations. Overall, the observed FT-IR features confirmed the presence of B-N, O-H, N-H, B-O, and B-C functionalities in the synthesized BNCQDs and supported the successful surface modification of the carbon quantum dots.

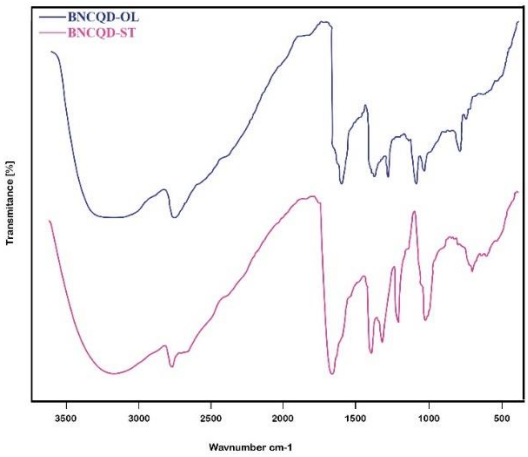

Figure 4. FT-IR of BNCQD-OL and BNCQD-ES.

3.2. XRD analyze

The crystalline structure of the synthesized samples was investigated by X-ray diffraction over the 2θ range of 5-60°. As shown in Figure 3, both CQDs and BNCQDs exhibited a single broad diffraction peak centered at approximately 2θ = 23.2°. This peak was assigned to the (002) diffraction plane of carbon-based materials and indicates the predominantly amorphous or poorly graphitized structure of the synthesized carbon quantum dots. The broadness of the diffraction peak reflects the low degree of crystallinity and the presence of structural disorder within the carbon framework. In addition, the incorporation of nitrogen and boron atoms, together with oxygen-containing surface functional groups, may increase the interlayer spacing by disrupting the regular stacking of the carbon layers. Similar increases in interplanar distance have been reported for nitrogen-doped graphitic materials [26]. Therefore, the observed broad peak and its position support the successful formation of heteroatom-doped carbon

quantum dots with an amorphous carbonaceous structure.

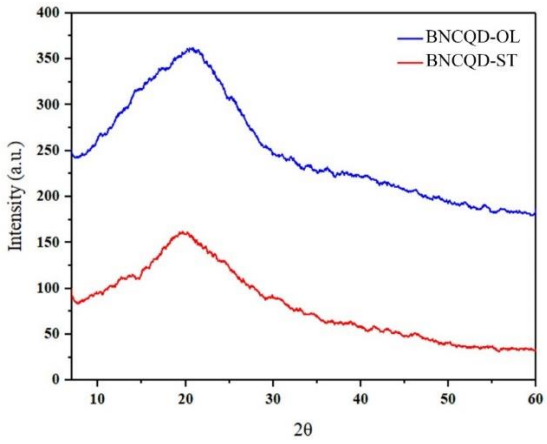

Figure 5. XRD patterns of BNCQD samples

3.3. Fluorescence analysis

Heteroatom doping is an effective strategy for tuning the photoluminescence (PL) properties of carbon quantum dots. Elements such as nitrogen, sulfur, and phosphorus can modify the electronic structure, surface states, and radiative recombination pathways of CQDs. Among these dopants, nitrogen has been studied extensively because nitrogen-containing surface and lattice sites can enhance PL emission by introducing additional electronic states and modifying the Fermi level. In particular, nitrogen atoms bonded to the carbon framework are considered important contributors to the enhanced fluorescence of N-doped CQDs [8, 27]. The fluorescence behavior of BNCQDs is also influenced by their surface functional groups. Carboxyl, hydroxyl, amino, and other oxygen- or nitrogen-containing groups generate surface energy states that affect electron-hole recombination and emission intensity. Therefore, variations in surface composition and functionalization may produce differences in emission wavelength and fluorescence intensity between the modified samples.

Fluorescence measurements were performed using an excitation wavelength of 357 nm and a spectral slit width of 1.6 nm. As shown in Figure 4, the BNCQD-OL sample exhibited a maximum emission peak at approximately 503 nm, whereas BNCQD-ST showed a maximum emission peak at approximately 585 nm. The shift in the emission maximum suggests that surface modification with oleic and stearic acids altered the surface states and local electronic environments of the BNCQDs. The longer-wavelength emission observed for BNCQD-ST may be attributed to differences in surface passivation, functional-group distribution, and the degree of electronic conjugation. Overall, the fluorescence results confirm that the optical properties of BNCQDs can be modulated through surface modification.

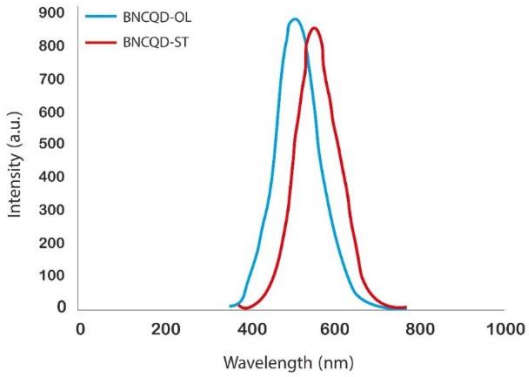

Figure 6. PL emission spectra of BNCQD-ST and BNCQD-OL

3.4. TGA

The thermal stability and decomposition behavior of the synthesized BNCQDs were investigated by thermogravimetric analysis under a nitrogen atmosphere at a heating rate

of 10 ℃ min^{-1}. As shown in Figure 5, the TGA curve of BNCQD-ST exhibited two main mass-loss stages. The first stage, corresponding to a weight loss of approximately 0.83%, was attributed to the removal of physically adsorbed water and residual volatile solvents. The second and major decomposition stage occurred at approximately 360 ℃ and resulted in a weight loss of about 96.4%. This substantial mass loss was associated with the thermal degradation of the organic surface groups and decomposition of the carbonaceous framework containing C-N and B-N functionalities.

The BNCQD-OL sample exhibited relatively high thermal stability and showed no substantial mass loss below approximately 350 ℃. A minor mass variation observed near 215 ℃ may be attributed to the desorption of adsorbed moisture or residual low-molecular-weight compounds. The principal decomposition stage occurred at approximately 350 ℃, resulting in a total weight loss of about 96.0%. Overall, both samples demonstrated comparable decomposition temperatures, indicating that the synthesized BNCQD derivatives remained thermally stable up to approximately 350 ℃. This level of thermal stability supports their potential application as lubricant additives under moderately elevated operating temperatures.

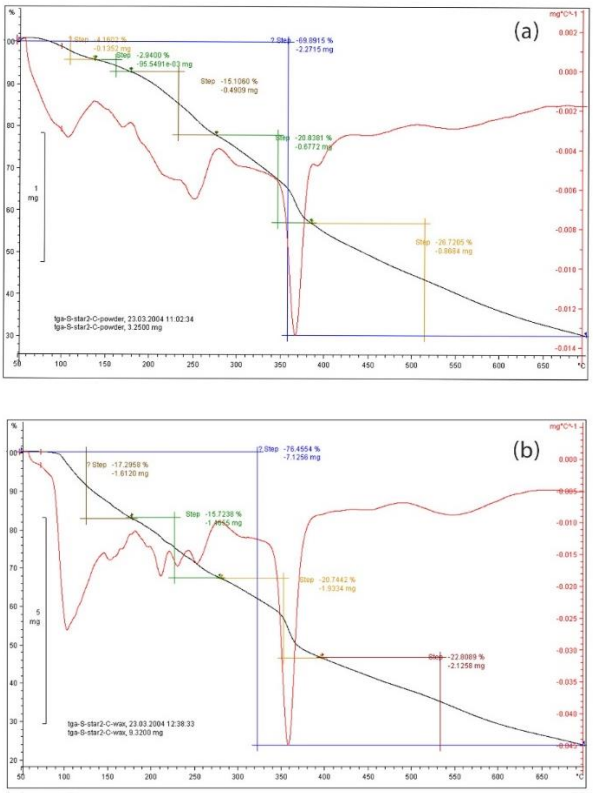

Figure 7. TGA curves of BNCQDs. (a) depicts the BNCQD-STs curve and (b) BNCQD-OL .

	Viscosity (cSt) at 40℃	Viscosity (cSt) at 100℃	Flash point (℃)	Pour point (℃)
BNCQD-OL	49.2	11.6	205.7	+39
BNCQD-ES	46.3	9.5	154	+23

Table 1. The main physical properties of these two BNCQDs are collected

3.5. ^{1}H NMR characterization

The ^{1}H NMR spectra of the synthesized BNCQDs are presented in Figure 9. The spectra showed several proton signals in the range of approximately 0.78-4.13 ppm,

indicating that most of the detectable protons were associated with aliphatic environments rather than aromatic or vinylic structures. These resonances may be assigned to alkyl, hydroxyl-bearing, and heteroatom-substituted carbon groups present on the surface of the carbon quantum dots. A weak signal was also observed at approximately 7.58 ppm, which may be attributed to aromatic or conjugated proton environments. However, the low intensity and small integral of this peak suggest that aromatic protons constituted only a minor fraction of the overall proton population. This observation is consistent with a predominantly aliphatic surface structure containing oxygen- and nitrogen-bearing functional groups.

The presence of signals in the downfield aliphatic region may also indicate proton environments adjacent to amide, amine, hydroxyl, or ester functionalities. These groups are expected to originate from the precursor molecules and the subsequent surface modification reactions. The abundance of hydroxyl and other polar functional groups improves the dispersibility of the BNCQDs in polar solvents such as water, methanol, and ethanol, whereas their compatibility with nonpolar solvents such as chloroform and toluene remains limited. Overall, the ^{1}H NMR results support the presence of predominantly aliphatic surface moieties together with a small proportion of aromatic or conjugated domains in the synthesized BNCQDs.

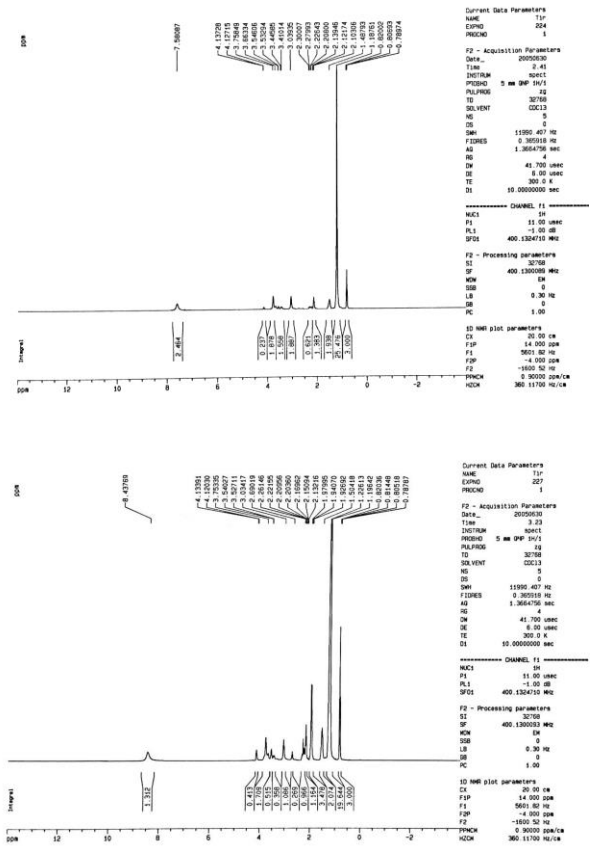

Figure 9. ^{1}H NMR of BNCQDs. (a) BNCQD-STs and (b) BNCQD-OL.

4. Conclusion

In this study, boron- and nitrogen-co-doped carbon quantum dots (BNCQDs) were successfully synthesized through a simple one-step thermal carbonization process using citric acid as the carbon source, boric acid as the boron source, and diethanolamine as the nitrogen source. The synthesized BNCQDs were subsequently modified with oleic acid and stearic acid to improve their compatibility with lubricant media. The structural and physicochemical analyses confirmed the formation of heteroatom-doped carbon quantum dots with abundant oxygen-, nitrogen-, and boron-containing functional groups. FT-IR spectroscopy indicated the presence of B-N, B-O, B-C, O-

H, N-H, and C-O functionalities, while XRD analysis revealed a broad diffraction peak centered at 2θ = 23.2°, characteristic of a predominantly amorphous carbon structure. The calculated interlayer spacing of the BNCQDs was greater than that of graphite, which may be attributed to heteroatom doping, structural disorder, and the presence of surface functional groups.

The synthesized samples also exhibited favorable optical and thermal properties. BNCQD-OL and BNCQD-ST showed distinct fluorescence emission maxima, indicating that surface modification influenced their electronic and surface states. Thermogravimetric analysis demonstrated that both derivatives remained relatively stable up to approximately 350 ℃, supporting their potential use under moderately elevated operating temperatures. In addition, the antioxidant results suggested that the synthesized BNCQDs possessed free-radical scavenging activity and could contribute to improved oxidative stability in lubricant formulations. Overall, the developed synthesis route was straightforward, cost-effective, and relatively mild. The combination of tunable surface chemistry, fluorescence behavior, thermal stability, antioxidant activity, and potential lubricant compatibility indicates that BNCQDs may serve as promising multifunctional additives for PEG-based lubricants. However, further tribological investigations, including friction, wear, load-carrying capacity, long-term dispersion stability, and comparison with commercial lubricant additives, are required before practical application.

Acknowledgments

The authors gratefully acknowledge the Chemistry Department, Faculty of Science, Azarbaijan Shahid Madani University, Tabriz, Iran, for providing the laboratory facilities and technical support required for this research.

Funding

This research received no external funding.

Declaration of Competing Interest

The authors declare that they have no known competing financial interests or personal relationships that could have influenced the work reported in this paper.

Data Availability Statement

The data supporting the findings of this study are available from the corresponding author upon reasonable request.

Reference

1. Wang, C.; Sun, Q.; Li, C.; Tang, D.; Shi, H.; Liu, E.; Guo, P.; Xue, W.; & Fan, J. Mater. Res. Bull. 2022, 155, 111970. DOI: 10.1016/j.materresbull.2022.111970.

2. Sabzi, F. E.; Assadi, M. G.; Valizadeh, H.; & Abdolmohammad-Zadeh, H. Water Air Soil Pollut. 2026, 237, 738. DOI: 10.1007/s11270-026-09371-x.

3. Deng, Y.; Long, Y.; Song, A.; Wang, H.; Xiang, S.; Qiu, Y.; Ge, X.; Golberg, D.; & Weng, Q. ACS Appl. Mater. Interfaces 2023, 15, 17045-17053. DOI: 10.1021/acsami.3c01705.

4. Liu, Y.; Li, W.; Wu, P.; Ma, C.; Wu, X.; Xu, M.; Luo, S.; Xu, Z.; & Liu, S. Sens. Actuators B Chem. 2019, 281, 34-43. DOI: 10.1016/j.snb.2018.10.075.

5. Huang, H.; Li, C.; Zhu, S.; Wang, H.; Chen, C.; Wang, Z.; Bai, T.; Shi, Z.; & Feng, S. Langmuir 2014, 30, 13542-13548. DOI: 10.1021/la503969z.

6. Sabzi, F. E.; Assadi, M. G.; Valizadeh, H.; & Abdolmohammad-Zadeh, H. Environ. Sci. Pollut. Res. 2026, 33, 9978-9999. DOI: 10.1007/s11356-026-37944-0.

7. Kim, K. H.; & Ahn, H. J. Int. J. Energy Res. 2022, 46, 8367-8375. DOI: 10.1002/er.7738.

8. Patra, R.; Panda, P. K.; Hung, C.-Y.; Dash, P.; Yang, P.-C.; & Hsieh, C.-T. Mater. Res. Bull. 2024, 180, 113040. DOI: 10.1016/j.materresbull.2024.113040.

9. Ustun, O.; Karadag, S. N.; Mazlumoglu, H.; Yilmaz, A.; & Yilmaz, M. Coatings 2023, 13, 456. DOI: 10.3390/coatings13020456.

10. Yadav, R.; & Lahariya, V. J. Fluoresc. 2025, 35, 12767-12780. DOI: 10.1007/s10895-025-04487-5.

11. Wang, Y.; Hu, X.; Li, W.; Huang, X.; Li, Z.; Zhang, W.; Zhang, X.; Zou, X.; & Shi, J. Spectrochim. Acta A Mol. Biomol. Spectrosc. 2020, 243, 118807. DOI: 10.1016/j.saa.2020.118807.

12. Liu, H.; Liu, Z.-H.; Zhang, J.; Zhi, L.; & Wu, M. New Carbon Mater. 2021, 36, 585-593. DOI: 10.1016/S1872-5805(21)60043-4.

13. Li, J.; Dong, Y.; Zhu, J.; Wang, L.; Tian, W.; Zhao, J.; Lin, H.; Zhang, S.; Cao, Y.; Song, H.; & Jia, D. Appl. Surf. Sci. 2020, 529, 147239. DOI: 10.1016/j.apsusc.2020.147239.

14. Zhang, Y.; Qin, H.; Huang, Y.; Zhang, F.; Liu, H.; Liu, H.; Wang, Z. J.; & Li, R. J. Mater. Chem. B 2021, 9, 4654-4662. DOI: 10.1039/D1TB00371B.

15. Yan, K.; Liu, X.; Kang, W.; Kalimuthu, R.; Ye, S.; & Feng, J. Opt. Mater. 2026, 173, 117846. DOI: 10.1016/j.optmat.2026.117846.

16. Kandasamy, G. C 2019, 5, 24. DOI: 10.3390/c5020024.

17. Zhang, X.; Wu, M.; Hou, A.; & Gao, A. ACS Appl. Nano Mater. 2024, 7, 13501-13511. DOI: 10.1021/acsanm.4c01800.

18. Dadkhah, S.; Mehdinia, A.; Jabbari, A.; & Manbohi, A. Microchim. Acta 2020, 187, 569. DOI: 10.1007/s00604-020-04543-w.

19. Liu, H.; Du, K.; Sun, H.; & Li, H. Res. Chem. Intermed. 2023, 49, 4291-4316. DOI: 10.1007/s11164-023-05106-3.

20. Wei, Y.; Chen, L.; Wang, J.; Liu, X.; Yang, Y.; & Yu, S. Opt. Mater. 2020, 100, 109647. DOI: 10.1016/j.optmat.2019.109647.

21. Li, G.; He, W.; Yan, R.; Cen, C.; Tan, X.; He, Y.; Wu, D.; & Huang, Y. Talanta 2025, 294, 128279. DOI: 10.1016/j.talanta.2025.128279.

22. Marvi, P. K.; Das, P.; Ganguly, S.; Tang, X. S.; Srinivasan, S.; & Rajabzadeh, A. R. ACS Appl. Polym. Mater. 2026, 8, 1777-1794. DOI: 10.1021/acsapm.5c03885.

23. Samarasiri, M. H.; Chandrasiri, T. A.; Wijesinghe, D. B.; & Gunawardena, S. P. Int. J. Food Eng. 2019, 5, 293-299. DOI: 10.18178/ijfe.5.4.293-299.

24. Das, R. K.; & Mohapatra, S. J. Mater. Chem. B 2017, 5, 2190-2197. DOI: 10.1039/C6TB03141B.

25. Chinigar, A. O.; Shomali, A.; & Valizadeh, H. Org. Commun. 2020, 13, 9-18. DOI: 10.25135/acg.oc.76.20.01.1530.